



ISSN: 0067-2904

## Spatiotemporal Variability and Trend of Ozone Pollution from Satellite Data (2003- 2021) in Iraq

Maha S. Hachim<sup>1\*</sup>, Jasim M. Rajab<sup>1</sup>, Ali M. Al-Salihi<sup>1</sup> and Hwee San Lim<sup>2</sup>

<sup>1</sup>Department of Atmospheric Science, Mustansiriyah University, Baghdad, Iraq

<sup>2</sup>School of Physics, University Sains Malaysia, 11800 Penang, Malaysia

Received: 27/9/2023

Accepted: 2/8/2024

Published: 15/11/2024

### Abstract

Ozone (O<sub>3</sub>) occurs naturally in the Earth's upper atmosphere, and at ground level is a dangerous pollutant that hurts plants and lung tissue and it's a major component of smog. The purpose of this study is to analyze the time series, trend, and spatial-temporal changes of monthly Relative Humidity (RH), Outgoing Longwave Radiation (OLR), and O<sub>3</sub> in Iraq using the Atmospheric Infrared Sounder (AIRS) ascending AIRS3STM data during 2003 - 2021. The time series over six stations (Mosul, Sulaymaniyah, Khanaqin, Rutba, Baghdad, and Basra) have been analyzed and showed similar changes and fluctuation in O<sub>3</sub> and OLR. The results of the study obtained were: minimum (decreasing, January–December) and maximum (increasing, May–August), and the mean and standard deviation were (0.044±0.003 ppmv) for O<sub>3</sub> and (298± 22 Wm<sup>-2</sup>) for OLR during the study period. During December to February, the highest RH values were recorded, while the lowest RH values occurred from June to August. The monthly mean and standard deviation of RH was (28.66±29.54 g/kg). Further O<sub>3</sub> trends revealed negative results in their annual series over all stations, except for Khanaqin and Basra, which had a positive trend. The O<sub>3</sub> concentrations were consistently connected with other meteorological variables (the O<sub>3</sub> has a negative correlation with RH and a beneficial correlation with temperature). The O<sub>3</sub> spatiotemporal maps showed recorded the highest values recorded in April and May over Mosul and Sulaymaniyah (0.055–0.057), and in December, at middle and southern regions (Baghdad and Basra), there were the lowest O<sub>3</sub> value (0.033). These results were due to meteorological and geographical factors. The results showed the efficient use of AIRS data to analyze the variations and distributions of atmospheric factors over different regions. In addition, AIRS observations can be used to obtain atmospheric, climatic, and environmental scientific reports and analyses for large, regional, and global regions and for long, continuous periods.

**Keywords:** Ozone (O<sub>3</sub>), Pollution, Trend, AIRS, Iraq.

التباين الزمني المكاني واتجاه تلوث الأوزون من بيانات الأقمار الصناعية (2003 - 2021) في

العراق

مها سلطان حاجم<sup>1\*</sup>، جاسم محمد رجب<sup>1</sup>، علي محمد الصالحي<sup>1</sup>، ليم سان هيوو<sup>2</sup>.

<sup>1</sup> علوم الجو، كلية العلوم، الجامعة المستنصرية، بغداد، العراق.

<sup>2</sup> مدرسة الفيزياء، جامعة سباز ماليزيا، 11800 بينانج، ماليزيا.

\*Email: [maha.alsultan89@gmail.com](mailto:maha.alsultan89@gmail.com)

## الخلاصة

حدث الأوزون ( $O_3$ ) بشكل طبيعي في الغلاف الجوي العلوي للأرض، وعلى مستوى الأرض هو ملوث خطير يضرّ بالنباتات وأنسجة الرئتين وهو مكون رئيسي في الضباب الدخاني. هدف هذه الدراسة تحليل السلسلة الزمنية، والاتجاه، والتغيرات المكانية-الزمانية للرطوبة النسبية الشهرية (RH)، والإشعاع الطويل المنبعث (OLR)، والأوزون في العراق باستخدام بيانات مسجل الأشعة تحت الحمراء الجوية (AIRS) AIRS3STM المتصاعدة خلال الفترة 2003 - 2021. تم تحليل السلسلة الزمنية عبر ست محطات (الموصل، السليمانية، خانقين، الرطبة، بغداد، والبصرة) وأظهرت تغيرات وتذبذب مماثلة في الأوزون وال-OLR. النتائج التي تم الحصول عليها كانت: الحد الأدنى (انخفاضات، كانون الثاني - كانون الأول) والحد الأقصى (زيادات، ايار - اب)، وكانت المتوسط والانحراف المعياري ( $0.003 \pm 0.044$  جزء في المليون) للأوزون ( $22 \pm 298$  واط/م<sup>2</sup>) لـ OLR خلال فترة الدراسة.

خلال كانون الأول إلى شباط، تم تسجيل أعلى قيم للرطوبة النسبية، بينما حدثت أقل قيم للرطوبة النسبية من حزيران إلى اب. وكان المتوسط الشهري والانحراف المعياري للرطوبة النسبية ( $29.54 \pm 28.66$  غ/كغ). كشفت الاتجاهات الأخرى للأوزون نتائج سلبية في سلسلتها السنوية عبر جميع المحطات، باستثناء خانقين والبصرة التي كانت لها اتجاه إيجابي. كانت تراكيز الأوزون متصلة باستمرار مع المتغيرات الأخرى الأخرى صادية (الأوزون له تراكيب

سلبية مع RH وترابط ايجابي مع درجة الحرارة). تظهر خرائط الزمان والمكان للأوزون أعلى القيم المسجلة في نيسان وإيار فوق الموصل والسليمانية ( $0.057-0.055$ ) ppmv، وفي كانون الأول، في المناطق الوسطى والجنوبية (بغداد والبصرة)، كانت أقل قيم الأوزون ( $0.033$ ) ppmv. تعود هذه النتائج إلى العوامل الأرصادية والجغرافية. أظهرت النتائج الاستخدام الفعال لبيانات AIRS لتحليل التغيرات والتوزيعات للعوامل الجوية عبر مناطق مختلفة. بالإضافة إلى ذلك، يمكن استخدام ملاحظات AIRS للحصول على تقارير وتحليلات علمية جوية ومناخية وبيئية لمناطق كبيرة وإقليمية وعالمية ولفترات زمنية طويلة ومتواصلة.

## Introduction

Ozone ( $O_3$ ) plays a significant role in air pollution, as it has been associated with adverse health effects in humans and damage to trees, plants, and ecosystems. As greenhouse gases (GHGs) contributing to climate change, it can negatively impact plant growth, hinder development, and elevate vulnerability to pests and diseases. The potential consequences include rising temperatures and alterations in weather Patterns. Studying and monitoring the spatiotemporal variability and trend of ozone pollution is crucial for protecting public health, the environment, and climate, ensuring regulatory compliance, managing air quality, and informing policy decisions [1],[2],[3],[4],[5]. Numerous studies have been conducted in various countries to address concerns regarding surface ozone pollution. These countries include China, the UK, Europe, Brazil, Mexico, Japan, South Korea, Australia, and the United States [6],[7],[8],[9],[10],[11],[12],[13],[14]. Atmospheric gases may be either naturally occurring or man-made. On the ground level and naturally in the high atmosphere of the Earth,  $O_3$  is beneficial because it absorbs harmful ultraviolet radiation from the Sun but on the ground, it is a hazardous contaminant that harms the environment and living systems and is therefore a critical atmospheric trace gas [15], [16]. According to reports,  $O_3$  is a strong oxidant and the most prominent index material of photochemical smog, and it is one of the principal pollutants deteriorating air quality [17]. The atmosphere's vertical thermal structure may change due to short- to long-term variations in  $O_3$  [18]. Although it has a considerably shorter lifespan than Carbon Dioxide ( $CO_2$ ) (a few weeks), tropospheric  $O_3$  plays a key role in the phenomena of global warming and climate change [19].

Because the  $O_3$  is not immediately released into the air like other pollutants, it is particularly harmful to the ecosystem and is hard to forecast and regulate. The  $O_3$  is produced through intricate chemical processes in the atmosphere [20]. Photochemical reactions between

nitrogen oxides (NO<sub>x</sub>) and non-methane hydrocarbons (NMHC) are responsible for its formation [21]. Intense photochemical interactions between major pollutants (NO<sub>x</sub> and NMHC) are fostered by intense solar radiation and high temperatures, leading to elevated levels of O<sub>3</sub> on sunny days [22], [23]. This means that the effect of photochemical reactions leading to O<sub>3</sub> generation and destruction is heavily influenced by weather conditions [24], [25].

The shorter O<sub>3</sub> lifespan due to substantial sinks in the boundary layer in the lower troposphere is reflected by the fact that the ozone mixing ratio rises with altitude. Since O<sub>3</sub> may be carried over long distances by the wind, the total amount of ozone in the air at any given point is the sum of that created locally and that carried there by the wind [17]. Atmospheric parameters have effect on O<sub>3</sub> concentration, it was found that the increase in O<sub>3</sub> value is associated with increase in the value of temperature and with drop in the levels of H<sub>2</sub>O<sub>vapor</sub> and RH [22]. The OLR plays a crucial role in providing a quantitative understanding of Earth's climate, specifically in relation to the radiative energy budget at the top of the atmosphere (TOA). Any changes in this essential component can lead to a prolonged imbalance in the net flux, ultimately influencing the climate as it undergoes adjustments to restore equilibrium. The OLR under clear-sky conditions depends on various factors, such as Earth's surface temperature, atmospheric temperatures, and the presence of absorbing gases. It arises from a combination of surface emissions and contributions from specific atmospheric layers [26].

There are several ways in which satellite data is essential to the research of pollutants: total protection, online tracking in real time satellites may give long-term data on pollutants, allowing researchers to investigate changes in pollutant levels over longer periods of time, and with a high degree of precision. This is especially helpful for determining how much damage pollution is doing to ecosystems and people, as well as how well pollution regulations are working. Analyzing information from many wavelengths: the temperature, content, and distribution of contaminants, as well as other useful information, may be gleaned from satellite data collected at different wavelengths (including visible, infrared, and microwave) [27], [28].

The AIRS instrument, data utilized in this work, is one of the six devices on NASA satellites (Aqua). It became a more useful device for researchers to observe atmospheric gas parameters and phenomena due to its free downloadable data from the NASA website. The AIRS is combined with the Advanced Microwave Sounding Unit (AMSU) to produce global meteorological datasets and atmospheric parameters (gases) at different standard levels using satellite data (AIRS) Level 3 Monthly Products (AIRX3STM) (daytime/ascending 1x1 degree resolution) Version 7, which involves 58 grid points of data covering all of Iraq [29]. Due to its effects on the troposphere's ability to oxidase, O<sub>3</sub> is recognized to be a substantial pervasive atmospheric trace gas that impacts the climate and contributes as an essential GHGs. This study aims to examine the monthly time series distribution of tropospheric O<sub>3</sub>, RH and OLR over six stations: Mosul, Sulaymaniyah, Khanaqin, Rutba, Baghdad, and Basra, for the entire study period (from January 2003 until December 2021). Also analyze the spatio-temporal and trend variations of O<sub>3</sub> across Iraq for the study period.

## 2. Materials and Methods

### 2.1. Study Area

The central part of the Asian nation of Iraq is between 38° and 49° East longitudes and 28° and 38° North latitudes. Geographically speaking, Iraq was shaped like the pelvis, with lofty mountains wrapping around it from the north to the northeast. In addition, the country is split

into three distinct regions: the desert in the west and southwest, the middle and southeast plains, featuring reedy wetlands in the southern region, and the highlands along the Euphrates and Tigris rivers [31]. Iraq, which lies in the Eastern Mediterranean, has a climate that falls somewhere between a continental and a subtropical and semi-arid one. In the winter, frigid Siberian and subtropical high-pressure systems move over Iraq, while the monsoon Asian low is the central synoptic system. Iraq experiences all four seasons and is subject to three different climatic regimes. Low-pressure systems originate throughout Asia during the summer monsoon season. The effects of the low monsoon are usually weakest during the winter, while its development has the most noticeable effects throughout the summer. Seasonal rains fall throughout much of Iraq from November to April, with precipitation levels varying from 1200 mm (millimeters) in the northeast to below 100 mm in 60% of the southern part of the country. Summertime rainfall is sporadic due to the prevalence of monsoon lows and common subtropical high-pressure systems. The hottest months of the year in the nation are July and August in the desert areas, when average midsummer temperatures top out at roughly 48 °C. Daytime highs in the winter average 16 degrees Celsius, but overnight lows may drop to 2 degrees Celsius, which is just over freezing. The coldest month is January, with temperature fluctuations between 5°C and 10°C [33].

## 2.2 Data Collection and Methodology

Environmental scientists are increasingly depending more and more on satellite remote sensing to collect data on atmospheric composition and climate change on a worldwide scale. For numerous atmospheric gases, their spectral radiance was resolved with high quality by the AIRS instrument on NASA's AQUA satellite. These data may be used to pinpoint the origins and sinks of GHGs emissions, as well as detect climate change. Data used in this study came from the AIRS Level-3 ascending data (<http://disc.sci.gsfc.nasa.gov/AIRS>) with a spatial resolution 1 x 1degree for six stations (Mosul, Sulaymaniyah, Khanaqin, Rutba, Baghdad, and Basra) as shown in Figure 1. The goals of the AIRS instrument are to get new information on the water and energy cycle and numerous GHGs, and to gain understanding into the weather and climate trends of the 21st century[31],[32].

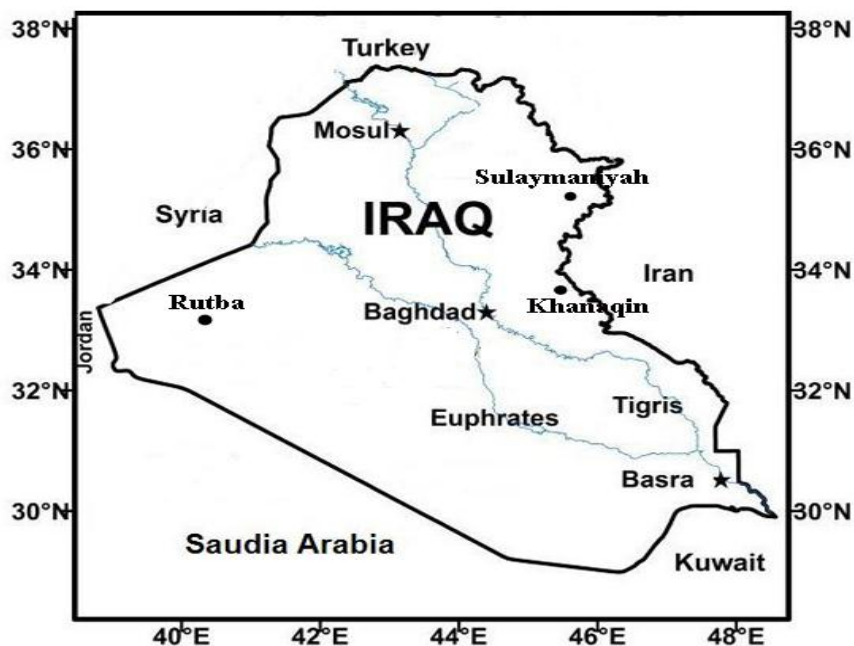


**Figure 1:** Ozone monitoring stations for locations (Mosul, Rutba, Khanaqin, Baghdad and Basra) in Iraq.

The AIRS was designed specifically to monitor the most crucial indicators of climate change. Aqua satellite, launched on May 4, 2002, mission incorporates the hyper-spectral thermal infrared radiometer AIRS. NOAA and NCEP research programmers created it to aid in climate-related studies and improve numerical weather prediction. With a 1650 km scanning swath, with a nadir field-of-view spatial resolution of 13.5 km and a ground track repeatability of +/- 20 km, comprehensive global coverage is provided twice daily. From the AIRS observed IR spectrum radiances, daytime and nocturnal ozone profiles in the 9.6-m region are derived [34],[35],[36].

To obtain the essential results of the present study, and to enhance our understanding of the O<sub>3</sub>, RH, and OLR fluctuations; the AIRS Level-3 (L3) ascending AIRS3STM (O<sub>3</sub>\_VMR\_A, RelHum\_A, and OLR\_A) data was employed. Generally, 228 monthly ascending granules (from January 2003 to December 2021, based on data availability) were acquired from the AIRS website in the form of HDF-EOS4 File forms to get the required output. The data was altered and arranged in tables using the MS Excel formula. The trends and time series graphs were generated using the Sigma Plot 14.0 software for the six stations in addition to calculate the maximum, minimum, and standard deviation values, summarized in Table 1. The study periods and monthly spatial graphics were conducted using the Surfer software.

### 3. Result and Discussion

#### 3.1 Analysis of ozone data

Time-averaged maps and time series plots were employed to analyze the spatiotemporal variations in O<sub>3</sub> data. Figure 2 illustrates the O<sub>3</sub> and OLR and RH mixing ratios for the major Iraqi cities (Mosul, Sulaymaniyah, Khanaqin, Rutba, Baghdad, and Basra) during 19 years, from 2003 to 2021. Table 1 contains data on tropospheric ozone during selected period.

As depicted in Figure-2(a), the average monthly O<sub>3</sub> reached peak values in March, April, and May, while the lowest values are observed in December, January, and February across the six stations. Peak O<sub>3</sub> values, reaching 0.054 ppmv, were observed in April and May over Mosul and Sulaymaniyah, and 0.052 ppmv over Kkhanaqin, Rutba, and Baghdad. In contrast, the lowest

**Table 1:** Annually mean of O<sub>3</sub>, Maximum, and Minimum, standard deviations, Trend and the locations, for the study period (2003-2021).

Stations	Longitude (E°)	Latitude (N°)	Altitude (m)	O <sub>3</sub> (ppmv)				
				Annual Min	Annual Max	Annual Mean	Std. Deviation	Trend/ per year
Mosul	43.06	36.21	223	0.034	0.054	0.044	0.01	-0.53 <sup>10</sup> -5
Sulaymaniyah	45.26	35.33	843	0.036	0.054	0.045	0.009	-1.05 <sup>10</sup> -5
khanaqin	45.5	34.5	200	0.035	0.052	0.044	0.008	1.05 <sup>10</sup> -5
Rutba	40.28	33.03	630	0.035	0.052	0.044	0.008	-1.68 <sup>10</sup> -5
Baghdad	44.40	33.30	32	0.035	0.052	0.044	0.008	-0.68 <sup>10</sup> -5
Basra	47.78	30.30	2	0.034	0.049	0.042	0.007	0.35 <sup>10</sup> -5

values, ranging from 0.034 to 0.036 ppmv, were recorded in December over Mosul and Sulaymaniyah, respectively. Mosul and Sulaymaniyah exhibited the highest O<sub>3</sub> values, with Khanaqin, Rutba, and Baghdad following suit. Conversely, Basra recorded the lowest O<sub>3</sub> values, attributed to O<sub>3</sub> sink mechanisms [30].

In Figure-2(b), the Outgoing Long Radiation (OLR) values show a continuous increase starting from January, reaching its peak in July and August, and subsequently decreasing until December. The observed pattern in the OLR curve was uniform across all six stations and can be adequately explained by the cyclic variations in meteorological conditions, particularly those related to changes in surface temperature and cloud cover. The peak OLR values, reaching 369.40 W/m<sup>2</sup>, were observed in July and August at Rutba, characterized by its desert environment with limited cloud cover and elevated temperatures during the months of June, July, and August. The minimum values (229.98, 231.22) W/m<sup>2</sup> occurred in January over Mosul, Sulaymaniyah, and Khanaqin, mainly due to the significant prevalence of cloud cover. Additionally, there was a slight decrease in OLR values over the Basra stations during June, July, and August, indicated by the maintenance of relatively constant values (356.0, 361.22, 359.0) W/m<sup>2</sup>, respectively.

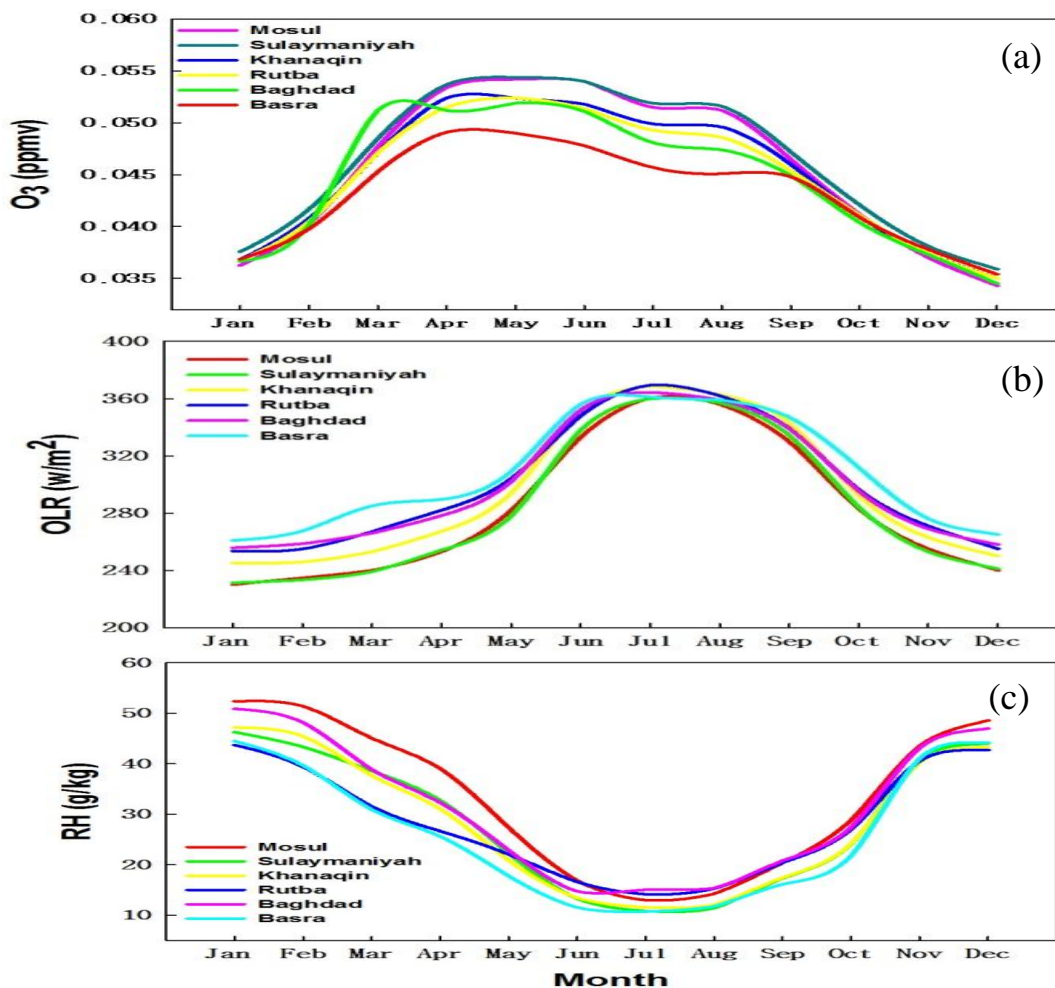


**Figure 2:** Mean monthly for a: ozone (ppmv), b: outgoing long radiation OLR (w/m<sup>-2</sup>) , c: relative humidity RH(g/kg)Values For six Selected Iraq Stations(2003 -2021).



In Figure 2 (c), Relative Humidity (RH) exhibited variations, with the highest values occurring in December, January, and February and the lowest from June to August at all stations. The peak value of 52.35 g/kg was recorded from December to February over Mosul, whereas the lowest value (10.71 g/kg) was observed from June to August over Basra. Examination of ozone data revealed that diverse weather conditions, including air temperature, shortwave radiation, air humidity, and topographical factors, significantly influence the variations in tropospheric O<sub>3</sub> over Iraq.

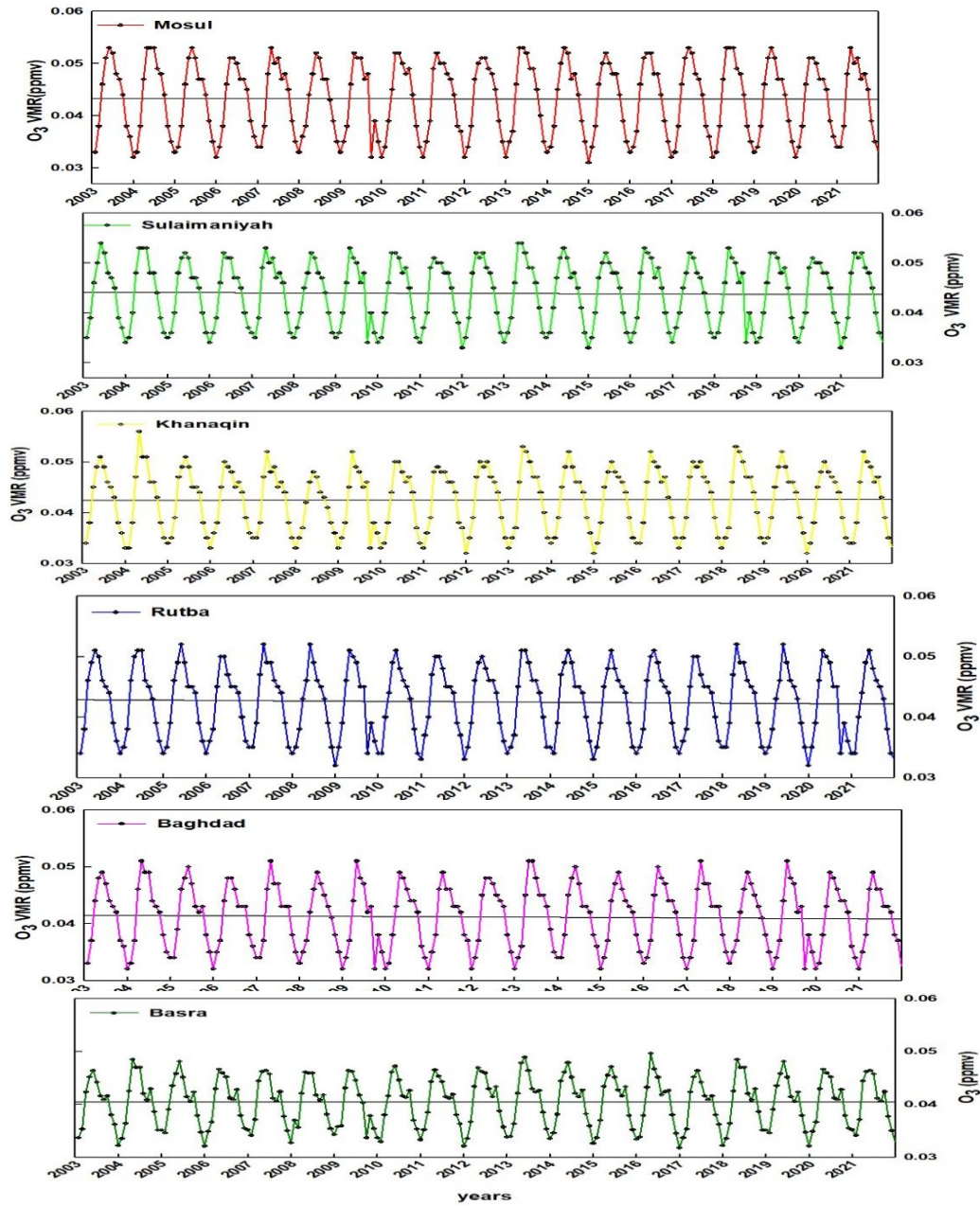


**Figure 3:** Time Series Analysis Ozone Volum Mixing Ratio concentration over Iraq (2003-2021)

The estimated trends and monthly time series for mean O<sub>3</sub> are depicted in (Figure 3) and (table 1), revealing a distinct monthly cycle with peaks in March - May and troughs in December - February for all stations considered. The periodic variation in climate and terrain

can adequately explain this behavior. The O<sub>3</sub> annual trends analysis was almost stable, with no statistically significant trend were be negative/decreasing ( $-0.53 \times 10^{-5}$ ) for Mosul station, ( $-1.05 \times 10^{-5}$ ) for Sulaymaniyah, ( $-1.68 \times 10^{-5}$ ) for Rutba, ( $-0.68 \times 10^{-5}$ ) for Baghdad and positive/increasing ( $1.05 \times 10^{-5}$ ) for Khanaqin, ( $0.35 \times 10^{-5}$ ) for Basra, show (table 1). The highest values observed (0.054 ppmv) during the period from March to May and the lowest values (0.032 ppmv) between December and January, The lowest values of O<sub>3</sub> can be interpreted as a direct effect of the O<sub>3</sub> sink by surface deposition where suitable conditions for photochemical loss (low temperature, low humidity, and low solar radiation) exist, the highest values of O<sub>3</sub> over higher latitude regions (Mosul, Sulaymaniyah, khanaqin, and Rutba), and a tendency to decrease downward to low latitude (Baghdad and Basra).

### 3.1.1 O<sub>3</sub> Spatiotemporal maps

For a more accurate assessment of the O<sub>3</sub> distribution over the Iraq region, the O<sub>3</sub> mean monthly data for the past 19 years (2003-2021) were used to map O<sub>3</sub>, as shown in Figure 4 the lowest value of O<sub>3</sub> in December witnessed the occurrence over Iraq followed by November in all regions of the country (0.032, 0.033) ppmv, while the highest values of O<sub>3</sub> record its occurrence in months (March – May) in April and May, the O<sub>3</sub> values were around (0.051 to 0.054) ppmv in the northern and northwestern regions (above latitudes 33.26°N), and approximately (0.046 to 0.049) ppmv in the remaining regions of Iraq, then begin to decline from June to August (0.049 to 0.052) ppmv.

The Ozone Maxing Ration (OMR) exhibited a typical distribution across Iraq throughout the year, following latitudinal gradients from north to south, with higher values for months with higher temperatures and lower values for months with lower temperatures and higher relative humidity. The variations in concentration OMR influenced by diverse weather conditions and topographical features, significantly impacting tropospheric ozone dynamics over Iraq. The considerable disparity in the values of OMR could be due to various effects, including variations in meteorological conditions, terrain, and the advection of pollutants from neighboring nations containing O<sub>3</sub> precursors emitted by human activity. To address the reduction of OMR emissions, firstly, efforts should focus on managing the emissions of Nitrogen Oxide (NO<sub>x</sub>) and Volatile Organic Compounds (VOCs) from diverse sources such as vehicles, industries, and power plants. Secondly, advocating for transportation strategies like public transit, carpooling, and cycling is crucial. Thirdly, implementing industrial controls and adopting cleaner production techniques are essential steps. Fourthly, promoting energy efficiency and transitioning towards renewable energy sources is imperative. Fifthly, incorporating land use and urban planning initiatives can help mitigate emissions. Sixthly, enforcing stringent emissions standards and regulations is necessary. Lastly, educating the public and fostering international collaboration are vital for achieving effective solutions.



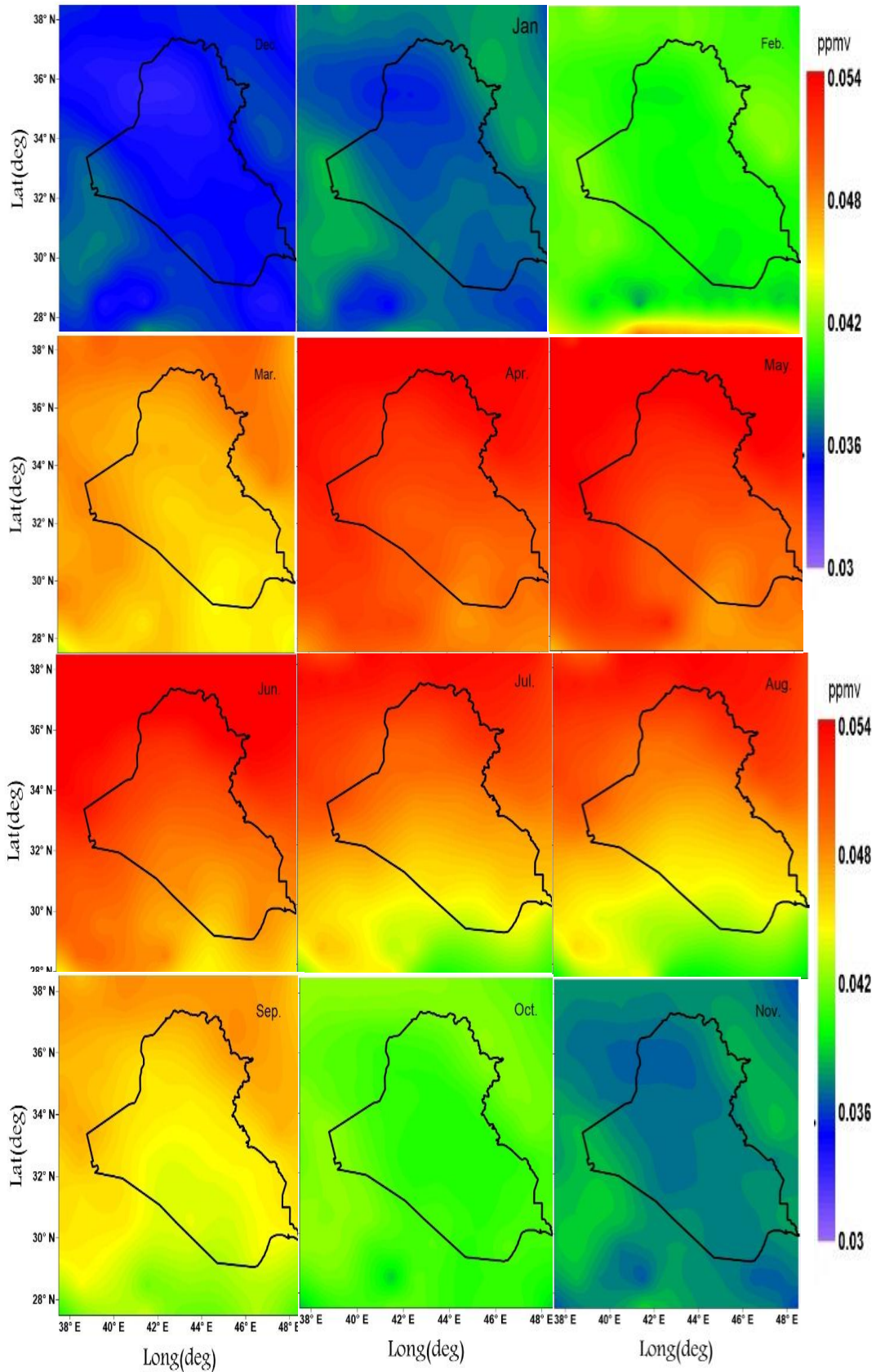


**Figure 4:** AIRS average monthly of Surface Ozone (O<sub>3</sub> VMR), over IRAQ for Summer (Jun - August) and Fall (September- November) seasons during 2003-2021.

#### 4. Conclusion

This work assessed the monthly troposphere O<sub>3</sub> VMR fluctuations throughout the study regions to perform in-depth studies of the temporal and geographical variability using the abundant information contained in nineteen years of satellite (AIRS) data (2003–2021). The results revealed significant spatiotemporal variability of O<sub>3</sub> value distribution across the research regions, with (mean ± SD) monthly readings of (0.044 ± 0.002) ppmv at the study period. In April and May, the highest concentrations of averaged surface O<sub>3</sub> VMR were Detected in the northern regions of Iraq at levels ranging from 51.35 to 51.75 ppmv near Mosul, while the lowest levels were observed in December in all of Iraq, particularly in the central and in the southern regions, the levels ranged from 31.67 to 32.22 ppmv in Baghdad and Basra. The O<sub>3</sub> yearly trends study showed a zonal variability with the greatest levels of O<sub>3</sub> across higher latitude locations (Mosul, Sulaymaniyah, Khanaqin, and Rutba) and a tendency to decline downhill to lower latitude regions (Baghdad and Basra) where attributed to O<sub>3</sub> sink mechanisms (such as Chlorofluorocarbons CFCs) through surface deposition and the more pronounced gaseous emissions from the petroleum refinery in Basra city. OLR values exhibited a continuous increase starting from January, reaching their peak in July and August, and then gradually declining until December. This pattern in the OLR curve remained consistent across all six stations. RH also peak values during the months December to February and the lowest values from June to August at all stations. Analysis of ozone data showed that increase O<sub>3</sub> value with increase OLR and decrease RH over Iraq. The considerable disparity in the values of O<sub>3</sub> mixing ratio are due to various effects, including variations in meteorological conditions (temperature, precipitation, humidity), chemistry (associated with tropospheric photochemical activity), terrain and the advection of pollutants from neighboring nations containing O<sub>3</sub> precursors emitted by human activities.

#### References

- [1] J. Wei, Z. Li, K. Li, R. R. Dickerson, R. T. Pinker, J. Wang, et al., "Full-coverage mapping and spatiotemporal variations of ground-level ozone (O<sub>3</sub>) pollution from 2013 to 2020 across China," *Remote Sensing of Environment*, vol. 270, p. 112775, 2022.
- [2] S. Xu, C. Cui, M. Shan, Y. Liu, Z. Qiao, L. Chen, et al., "Spatio-temporal prediction of ground-level ozone concentration based on Bayesian maximum entropy by combining monitoring and satellite data," *Atmosphere*, vol. 13, p. 1568, 2022.
- [3] H. Liu, S. Liu, B. Xue, Z. Lv, Z. Meng, X. Yang, et al., "Ground-level ozone pollution and its health impacts in China," *Atmospheric environment*, vol. 173, pp. 223-230, 2018.
- [4] Y. Gu, K. Li, J. Xu, H. Liao, and G. Zhou, "Observed dependence of surface ozone on increasing temperature in Shanghai, China," *Atmospheric Environment*, vol. 221, p. 117108, 2020.
- [5] P. Liu, H. Song, T. Wang, F. Wang, X. Li, C. Miao, et al., "Effects of meteorological conditions and anthropogenic precursors on ground-level ozone concentrations in Chinese cities," *Environmental Pollution*, vol. 262, p. 114366, 2020.
- [6] S. Mousavinezhad, Y. Choi, A. Pouyaei, M. Ghahremanloo, and D. L. Nelson, "A comprehensive investigation of surface ozone pollution in China, 2015–2019: Separating the contributions from meteorology and precursor emissions," *Atmospheric Research*, vol. 257, p. 105599, 2021.
- [7] W. Li, Y. Wang, J. Flynn, R. J. Griffin, F. Guo, and J. L. Schnell, "Spatial variation of surface O<sub>3</sub> responses to drought over the contiguous United States during summertime: Role of precursor emissions and ozone chemistry," *Journal of Geophysical Research: Atmospheres*, vol. 127, no. 1, p. e2021JD035607, 2022.
- [8] E. Hertig, A. Russo, and R. M. Trigo, "Heat and ozone pollution waves in central and south Europe—characteristics, weather types, and association with mortality," *Atmosphere*, vol. 11, no. 12, p. 1271, 2020.
- [9] A. Boari, R. Pedruzzi, and M. Vieira-Filho, "Air pollution trends and exceedances: ozone and particulate matter outlook in Brazilian highly urbanized zones," *Environmental Monitoring and Assessment*, vol. 195, no. 9, p. 1058, 2023.

- [10] J. V. Santiago *et al.*, "Ozone responses to reduced precursor emissions: A modeling analysis on how attainable goals can improve air quality in the Mexico City Metropolitan Area," *Science of The Total Environment*, vol. 912, p. 169180, 2024.
- [11] J. Vazquez Santiago, K. Inoue, and K. Tonokura, "Modeling Ground Ozone Concentration Changes after Variations in Precursor Emissions and Assessing Their Benefits in the Kanto Region of Japan," *Atmosphere*, vol. 13, no. 8, p. 1187, 2022.
- [12] H.-M. Lee and R. J. Park, "Factors determining the seasonal variation of ozone air quality in South Korea: Regional background versus domestic emission contributions," *Environmental Pollution*, vol. 308, p. 119645, 2022.
- [13] R. G. Ryan, S. Rhodes, M. Tully, and R. Schofield, "Surface ozone exceedances in Melbourne, Australia are shown to be under NO<sub>x</sub> control, as demonstrated using formaldehyde: NO<sub>2</sub> and glyoxal: formaldehyde ratios," *Science of the Total Environment*, vol. 749, p. 141460, 2020.
- [14] M. Mitchell, A. Wiacek, and I. Ashpole, "Surface ozone in the North American pollution outflow region of Nova Scotia: Long-term analysis of surface concentrations, precursor emissions and long-range transport influence," *Atmospheric Environment*, vol. 261, p. 118536, 2021.
- [15] Y. Liu, "Research Progress and Trends in the Field of Satellite Ozone from 2005 to 2023: A Bibliometric Review," *Atmosphere*, vol. 14, no. 8, p. 1245, 2023.
- [16] T. Vandyck, K. L. Ebi, D. Green, W. Cai, and S. Vardoulakis, "Climate change, air pollution and human health," *Environmental Research Letters*, vol. 17, no. 10, p. 100402, 2022.
- [17] A.-C. Pinho-Gomes *et al.*, "Air pollution and climate change," *The Lancet Planetary Health*, vol. 7, no. 9, pp. e727-e728, 2023.
- [18] H.-M. Lee and R. J. Park, "Factors determining the seasonal variation of ozone air quality in South Korea: Regional background versus domestic emission contributions," *Environmental Pollution*, vol. 308, p. 119645, 2022.
- [19] R. G. Ryan, S. Rhodes, M. Tully, and R. Schofield, "Surface ozone exceedances in Melbourne, Australia are shown to be under NO<sub>x</sub> control, as demonstrated using formaldehyde: NO<sub>2</sub> and glyoxal: formaldehyde ratios," *Science of the Total Environment*, vol. 749, p. 141460, 2020.
- [20] M. R. Jasim, M. MatJafri, F. Tan, H. Lim, and K. Abdullah, "Analysis of Ozone column burden in Peninsular Malaysia retrieved from Atmosphere Infrared Sounder (AIRS) data: 2003–2009," 2011 IEEE International Conference on Imaging Systems and Techniques, 978-1-61284-896-9/11 IEEE, DOI: 10.1109/IST.2011.5962213, 2011, pp. 29-33.
- [21] J. Deng, Z.-Y. Zhang, Q. Yang, and X.-D. Wu, "Overview of non-methane volatile organic compounds for world economy: From emission source to consumption sink," *Energy Nexus*, vol. 6, p. 100064, 2022.
- [22] W. Li, Y. Wang, J. Flynn, R. J. Griffin, F. Guo, and J. L. Schnell, "Spatial variation of surface O<sub>3</sub> responses to drought over the contiguous United States during summertime: Role of precursor emissions and ozone chemistry," *Journal of Geophysical Research: Atmospheres*, vol. 127, no. 1, p. e2021JD035607, 2022.
- [23] J. Ding *et al.*, "Impacts of meteorology and precursor emission change on O<sub>3</sub> variation in Tianjin, China from 2015 to 2021," *Journal of Environmental Sciences*, vol. 126, pp. 506-516, 2023.
- [24] J. Vazquez Santiago, K. Inoue, and K. Tonokura, "Modeling Ground Ozone Concentration Changes after Variations in Precursor Emissions and Assessing Their Benefits in the Kanto Region of Japan," *Atmosphere*, vol. 13, no. 8, p. 1187, 2022.
- [25] M. Wang *et al.*, "Meteorological and anthropogenic drivers of surface ozone change in the North China Plain in 2015–2021," *Science of the Total Environment*, vol. 906, p. 167763, 2024.
- [26] M. Wondie and S. Abeje, "Modeling outgoing long-wave radiation based on the atmospheric moisture parameters and correlated to the air temperature in Ethiopia," *Climate Dynamics*, vol. 61, no. 3, pp. 1607-1623, 2023.
- [27] S. Dey, B. Purohit, P. Balyan, K. Dixit, K. Bali, A. Kumar, *et al.*, "A satellite-based high-resolution (1-km) ambient PM<sub>2.5</sub> database for India over two decades (2000–2019): applications for air quality management," *Remote Sensing*, vol. 12, p. 3872, 2020.
- [28] G. Kaplan and Z. Y. Avdan, "Space-borne air pollution observation from sentinel-5p tropomi: Relationship between pollutants, geographical and demographic data," *International Journal of Engineering and Geosciences*, vol. 5, pp. 130-137, 2020.

- [29] I. S. Abdulfattah, J. M. Rajab, M. Chaabane, M. H. Lafta and H. S. Lim, "Air Surface Temperature Variability and Trends from Satellite Homogenized Time Series Data Over Tunis 2003–2021", *IOP Conf. Ser.: Earth Environ. Sci.* 1223 012017, 2023.
- [30] R. Janardanan *et al.*, "Country-level methane emissions and their sectoral trends during 2009–2020 estimated by high-resolution inversion of GOSAT and surface observations," *Environmental Research Letters*, vol. 19, no. 3, p. 034007, 2024.
- [31] A. Mohammed and J. H. Kadhum, "Dynamical Study for Selective Extreme Events over Iraq and Their Relations with General Circulations," *Al-Mustansiriyah Journal of Science*, vol. 32, 2021.
- [32] M. Loveless *et al.*, "Comparison of the AIRS, IASI, and CrIS infrared sounders using simultaneous nadir overpasses: novel methods applied to data from 1 October 2019 to 1 October 2020," *Earth and Space Science*, vol. 10, no. 7, p. e2023EA002878, 2023.
- [33] F. S. Basheer, "Trend Analysis of Annual Surface Air Temperature for Some Stations over Iraq," *Al-Mustansiriyah Journal of Science*, vol. 33, pp. 77-82, 2022.
- [34] P. Rawat *et al.*, "Performance of AIRS ozone retrieval over the central Himalayas: use of ozonesonde and other satellite datasets," *Atmospheric Measurement Techniques*, vol. 16, no. 4, pp. 889-909, 2023.
- [35] L. Zhou *et al.*, "Spatiotemporal variability of global atmospheric methane observed from two decades of satellite hyperspectral infrared sounders," *Remote Sensing*, vol. 15, no. 12, p. 2992, 2023.
- [36] Z. Xu *et al.*, "Study of Methane Emission and Geological Sources in Northeast China Permafrost Area Related to Engineering Construction and Climate Disturbance Based on Ground Monitoring and AIRS," *Atmosphere*, vol. 14, no. 8, p. 1298, 2023.